# Multi-Decadal annual cycle variation, Monsoon and Teleconnections

**Yung-An Lee**

**Institute of Atmospheric Physics,**
**National Central University**

## Abstract

In this study, a multi-decadal annual cycle variation mode was identified from National Centers for Environmental Prediction / National Center for Atmospheric Research (NCEP/NCAR) reanalysis monthly mean data. Spectrum analysis revealed that this mode has two fundamental frequencies at both sides of the annual cycle. Due to interaction between these two frequencies, the mode exhibited strong multi-decadal amplitude and phase variation. its spatial-temporal evolution has intimate link to monsoon and major atmospheric teleconnection patterns. Furthermore, it showed that monsoon as well as Rossby wave propagation and reflection may play important role in establishing these teleconnection patterns. These results indicate that dynamic process is capable of generating multi-decadal variability in the atmosphere. Therefore, the anomalous climate of the past two decades does not necessarily imply global warming per se.

## Introduction

The anomalous change of climate in recent decades has attracted much attention of climate researches on interdecadal variability (e.g., Latif, Kleeman and Eckert, 1997; Wang, 1995). Whether it is a part of nature variability (Wallace, Zhang and Renwick, 1995) or a fingerprint of global warming (Graham, 1995; Kawamura et al., 1995) is still unclear. For climate variability of interannual timescales and beyond, oceanic variability or external forcing is generally believed to be the dominant mechanism to generate such variability. And yet, some studies (Wallace, Zhang and Lau, 1993; Wallace, Zhang and Bajuk, 1996) had shown that atmospheric interdecadal variability has distinct seasonality. Numerical modeling (James and James, 1989) had also shown that nonlinear process alone can generate interdecadal variability in the atmosphere. Considering the relatively fast adjustment timescale of the atmosphere, one may wonder just what kind of physical process can generate such low frequency variability?

It is well known that the interaction of two waves with nearby frequencies can generate a wave whose frequency is the mean of the two and whose amplitude is modulates by an envelop wave that has frequency equal to one-half the difference of the two, e.g.,

$$e^{i(k+\Delta k)t} + e^{i(k-\Delta k)t} = 2\cos(\Delta kt)e^{ikt}. \quad (1)$$

Thus, it is quite possible that two nearby dynamic induced high frequency modes can generate very low frequency variability. Then, the remaining question is, can we identify such phenomenon in observed data? To answer this question, one needs not only to identify the existence of a high frequency wave with its amplitude modulated by a low frequency envelop wave, but also needs to show that this signal has distinct physical identity. Obviously, traditional time series analysis can not provide enough information to adequately identify this kind of signal. In this study, I demonstrated that multi-channel singular spectrum analysis (MSSA; Plaut and Vautard, 1994; Zhang, Sheng and Shabbar, 1998; Vautard, Yiou and Ghil, 1992) is capable of identifying such phenomenon in NCEP/NCAR reanalysis data (Kalnay et al. 1996).

MSSA, briefly speaking, is an extension of the principal component analysis (PCA, Preisendorfer and Mobley 1988) of a time series of spatial vectors to include additionally analysis of temporal structure. This analysis can effectively extract oscillatory signals and differentiate variability associated with different timescales in data. To obtain coherent spatial-temporal structures among variables, monthly mean geopotential height, temperature, zonal wind, meridional wind, streamfunction and velocity potential fields between 1950 and 1998, from 1,000 to 150 hPa and $80^0$ S to $80^0$ N with $5^0$ longitudes by $5^0$ latitudes resolution were included in the analysis. The climate mean annual cycle was first removed and the resultant anomaly time series was then normalized by its own standard deviation at each grid. To compress these data, every normalized field at each level is subjected to a PCA to extract the leading 60 principal components (PCs). Then, another PCA is applied to all these retained PCs. Finally, a MSSA with 144-month window length is applied to the leading 30 of the resultant PCs to extract dominant spatial-temporal principal components (ST-PCs) and empirical orthogonal functions (ST-EOFs) of the atmosphere.

## Spatial-Temporal evolution of QAO

Figure 1**a** shows the explained variance of the leading 30 ST-PCs and their associated 99% confident intervals. The most interesting feature of this panel is that the 99% confident intervals of both ST-PC 11 and 12 have much lower upper bounds than other modes. Since an AR (1) process has no inherent oscillatory signal, this phenomenon indicates that these two modes are most likely a pair of oscillatory modes that represents a quasi- periodic signal of data. Panel **b** and **c** show the time evolution of these two modes. We can see that they evolve like a high frequency quasi-annual wave

modulated by a multi-decadal low frequency envelope wave. To examine this feature more closely, figures 2 shows, reconstructed from ST-PC 11 and 12 the time series of 1,000 hPa geopotential height field and its associated Fourier spectrum at $50^0$ N, $110^0$ E. The Fourier spectrum exhibits two sharp peaks at both sides of annual cycle, while the time series and the month-year diagram in panel a and c clearly show a nearly annual cycle oscillation with phase reversing around 35-40 years. Therefore, it appears that the interaction of these two nearby frequencies around annual cycle is the main mechanism in generating this quasi-annual oscillation (QAO) with multi-decadal variability.

To examine physical significance of this QAO signal, figure 3 shows a half cycle spatial-temporal evolution of geopotential height at 1,000 hPa. In January, dominant positive anomalies were found in East Asia and Atlantic Ocean north of $50^0$ N, while negative anomalies were seen in mid-Atlantic around $40^0$ N, Indian Ocean and Atlantic south of $50^0$ S. In February, anomalies in East Asia, southern Indian Ocean and northern Atlantic weakened, while those in east of Aleutian, tropical central Pacific, equatorial eastern Pacific and tropical Africa strengthened. The mid-Atlantic anomaly showed slightly northward propagation. During boreal spring, East Asia positive anomaly continued to weakened and finally replaced by negative anomaly that originated from middle of Eurasia continent. The mid-Atlantic negative anomaly and the positive anomaly near Aleutian also weakened but, at the same time, propagated respectively northward and southwestward to replace original northern Atlantic positive anomaly and western subtropical Pacific negative anomaly. During the same period, the negative anomaly in equatorial eastern Pacific predominantly moved southwestward and merged with negative anomaly from southern Indian Ocean near New Zealand. On the other hand, the tropical African positive anomaly gradually moved across Atlantic and developed relative strong center near southeast coast of United States. From May to June, a similar spatial pattern with opposite sign to that of January was established. Noted that the positive anomaly near Aleutian almost disappeared, while the western subtropical Pacific positive anomaly showed sign of moving east-southeastward toward Hawaii. The negative anomaly near New Zealand also moved eastward toward coast of South America, while center near southeast coast of US moved to central Atlantic south of $40^0$N. Spatial patterns of the other half cycle of QAO were almost the same as those of panel a to f, except for sign reversal. Therefore, panel f and a indicated that the anomaly near Aleutian was originated from East Asia. From this figure, three interesting features can be identified. First, the strong signal and phase reversal between boreal winter and summer seasons in East Asia suggest that QAO has a very close relation with the Eastern Asian monsoon. Second, North Atlantic Oscillation (opposite pressure anomalies between midlatitudes and high latitudes of Northern Atlantic, NAO) is observed all year round. In fact, we saw that this kind of pressure alterations occurred in the whole Atlantic Ocean. These results are consistent with those of previous studies (Barnston and Livezey, 1987; Hurrell and Van Loon, 1997, Xie and Tanimoto, 1998). Furthermore, it appears that these anomalies are all generated alternatively in tropical western Africa. As time progressed, they grew and moved eastward through tropical Atlantic toward southeast coast of US. Then, these anomalies gradually move north following seesaw-like path to establish the pressure alternation pattern in the northern Atlantic. It seems that, during northward propagation, these anomalies were reflected back and forth by US as well as western African coastlines. These features indicate that western African monsoon as well as Rossby wave propagation and reflection may play very important role in NAO mechanism. Third, in contrast with equatorial origin and predominantly northward propagation of anomalies in Northern Atlantic, anomalies in Northern Pacific had East Asia origin and had predominantly southward propagation. Nevertheless, they also followed seesaw-like path during southward propagation. Furthermore, it is noted that anomalous pressure alternation pattern from equatorial central Pacific to east of Aleutian resembles the Pacific part of surface pressure map of the familiar Pacific-North America (PNA; Wallace and Gutzler, 1981) teleconnection pattern. Therefore, East Asia monsoon as well as Rossby wave propagation and reflection may also play important role in PNA mechanism.

To examine closely the relation among QAO, PNA and NAO, figure 4 shows QAO evolution of the 500 hPa geopotential height field. In January, the anomaly center in Asian continent was moved from East Asia around $50^0$ N in 1,000 hPa southwestward to around Tibetan plateau. There was also a pair of opposite anomalies, which did not have clear counterpart in 1,000 hPa, appeared in southern Indian Ocean. They appeared to form a pair of standing oscillation because they showed no obvious propagation during the whole QAO cycle. In March, every center of PNA pattern clearly appeared in its respective region. The origins of individual centers of this pattern can be traced back to from anomalies in East Asia, Arctic regions, and equatorial Africa of previous months. This result suggests that both East Asia and western African monsoons have important influence on establishing PNA connection pattern. Note that NAO is still clearly visible in northern Atlantic all year round. The timing of the appearance of PNA and NAO is consistent with previous study (Barnston and Livezey, 1987). Furthermore, the all-year-round appearances of NAO pattern in spatial-temporal evolution of QAO also consistent with the existence of significant one-year lag-correlation of NAO (Hurrell and Van Loon, 1997)

## Summary and conclusion

In summary, although ST-PC 11 and 12 are not the most important modes that explained the most variance of the NCEP/NCAR reanalysis data, the above results indicated that QAO is a genuine and very important quasi-periodic signal of the atmosphere. It is noted that similar signal can be identified in ST-PC 4 and 5 if MSSA is applied to 1,000 hPa wind fields alone. The degrading of QAO signal in eigenvalue ranking shown in here is the price paid for obtaining coherent

spatial-temporal structures among various variables to examine its physical significance.

From spatial-temporal evolution of QAO we learned that it has close link with fluctuation of mean annual cycle. We also learned that East Asia and western African monsoons as well as Rossby wave propagation and reflection may play very important role in establishing PNA and NAO patterns. These results suggest that QAO may be a residue of the imbalance between annual radiative forcing and dynamical response of the atmosphere. Moreover, the multi-decadal modulation of amplitude and phase of QAO indicates that interdecadal variability can be generated by internal dynamics alone. Thus climate variability in recent decades does not necessarily imply the existence of low frequency external forcing or global warming per se.

This study also clearly demonstrated the ability of MSSA to extract nonlinear signal from data. Furthermore it showed the capability of spatial-temporal evolution in aiding our interpretation and identifying physically significant signal. It is noted that because QAO is constituted of two nearby frequencies around annual cycle, it can not be correctly identified if data had been low-pass filtered or had been seasonal stratified. Therefore this study also pointed out that improper filtering of data might distort and mask physically significant signals.

## References


Allen, M. R. and L. Smith, 1996: A. Monte Carlo SSA: Detecting irregular oscillations in the presence of colored noise. *J. Clim.*, **9**, 3373-3404.

Barnston, A. G. and R. E. Livezey, 1987: Classification, seasonality and persistence of low-frequency atmospheric circulation patterns. *Mon. Wea. Rev.*, **115**, 1083-1126.

Graham, N. E., 1995: Simulation of recent global temperature trends. *Science*, **267**, 666-671.

Hurrell, J. W. and H. Van Loon, 1997: Decadal variations in climate associated with the North Atlantic Oscillation. *Climate Change*, **36**, 301-326.

James, I. N. and P. M. James, 1989: Ultra-low-frequency variability in a simple atmospheric circulation model. *Nature*, **342**, 53-55.

Kalnay, E., et al., 1996: The NCEP/NCAR 40-year reanalysis project. *Bull. Amer. Meteor. Soc.*, 77, 437-471.

Kawamura, R., et al., 1997: Recent abnormal changes in wintertime atmospheric response to tropical SST forcing. *Geo. Res. Lett.*, **24**, 783-786.

Latif, M., R. Kleeman, and C. Eckert, 1997: Greenhouse warming, Decadal variability, or El Niño? An attempt to understand the anomalous 1990s. *J. Clim.*, **10**, 2221-2239.

Plaut, G. and R. Vautard, 1994: Spells of low-frequency oscillations and weather regimes in the Northern Hemisphere. *J. Atmos. Sci.* **51**, 210-236.

Preisendorfer, R. W. and C. D. Mobley, 1988: Principal Component Analysis in Meteorology and Oceanography, Elsevier, Amsterdam, 425 pp.

Vautard, R., P. Yiou and M. Ghil, 1992: Singular-spectrum analysis: A toolkit for short, noisy chaotic signals. *Physica D* **58**, 95-126.

Wallace, J. M. and D. S. Gutzler, 1981: Teleconnections in geopotential height field during the Northern Hemisphere winter. *Mon. Wea. Rev.* **109**, 784-812.

Wallace, J. M., Y. Zhang and K.-H. Lau, 1993: Structure and seasonality of interannual and interdecadal variability of the geopotential height and temperature fields in the Northern Hemisphere troposphere. *J. Clim.* **6**, 2063-2082.

Wallace, J. M., Y. Zhang, and A. Renwick, 1995: Dynamic contribution to hemispheric mean temperature trends. *Science* **270**, 780-783.

Wallace, J. M., Y. Zhang and L. Bajuk, 1996: Interpretation of interdecadal trends in Northern Hemisphere surface air temperature. *J. Clim.* **9**, 249-259.

Wang, B., 1995 Interdecadal changes in El Niño onset in the last four decades. *J. Clim.* **8**, 267-285.

Xie, S. -P. and Y. Tanimoto, 1998: A pan-Atlantic decadal climate oscillation. *Geo. Res. Lett.* **24**, 2185-2188.

Zhang, X., J. Sheng and A. Shabbar, 1998: Modes of interannual and interdecadal variability of Pacific SST. *J. Clim.* **11**, 2556-2569.

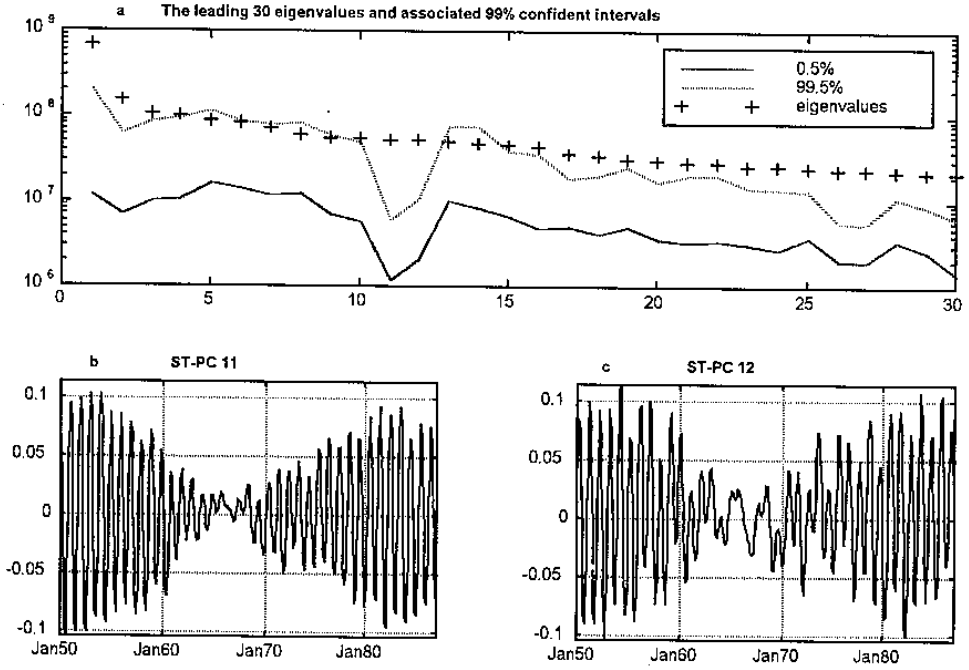


Figure 1. Panel **a** shows the explained variance of the leading 30 ST-PCs of MSSA. Also included are the 99% confident intervals that estimated from 200 Monte-Carlo MSSA simulations (Allen and Smith, 1996; Zhang, Sheng and Shabbar, 1998) of a red noise model that consists of 30 independent AR (1) processes, each with the same variance and first-order autocorrelation as those of the retained 30 PCs. Panel **b** and **c** show respectively the time evolutions of ST-PC 11 and 12. It is noted that, due to the 144-month window length, time series in panel **b** and **c** were ended at January 1987.

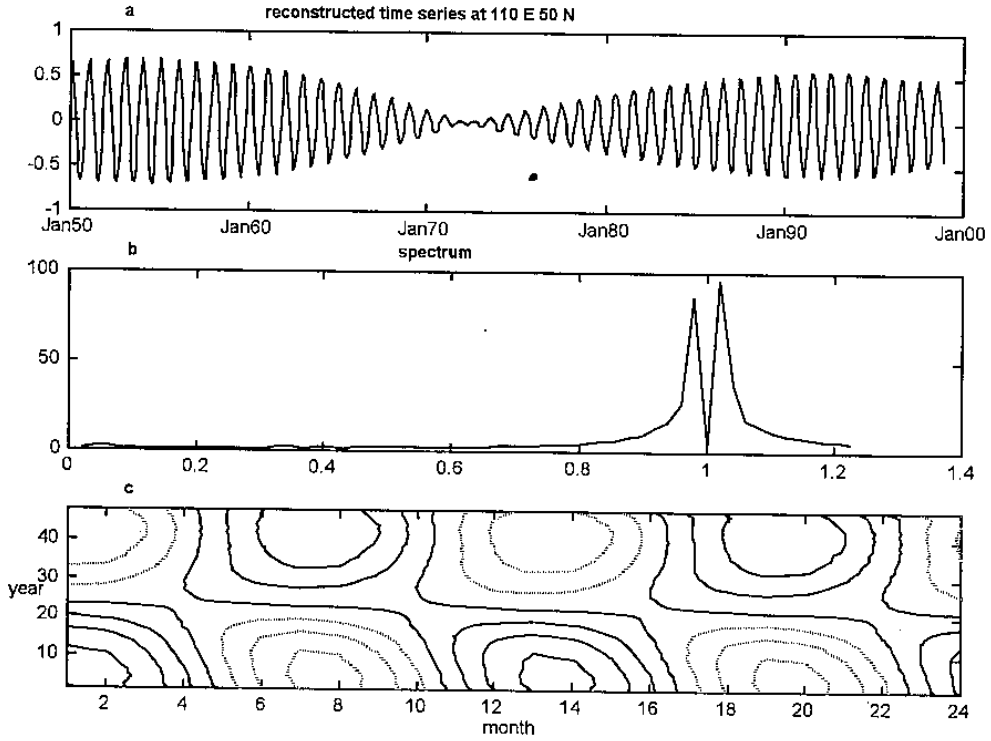


Figure 2. Panel **a** is the time series of 1,000 hPa geopotential height at 50° N and 110°E, reconstructed from ST-PC 11 and 12 and near the location of maximum variability. Panel **b** shows the corresponding Fourier spectrum (power vs. 1/year) of the reconstructed time series. Panel **c** shows the same reconstructed time series in the form of month-year diagram. It is noted that, to show more clearly the characteristics of QAO, the month-axis had been expanded to cover 24 months period. Therefore the year-axis was reduced by one to 48 years. This kind of presentation allows easily identifying QAO and its associated multi-decadal amplitude and phase modulation.

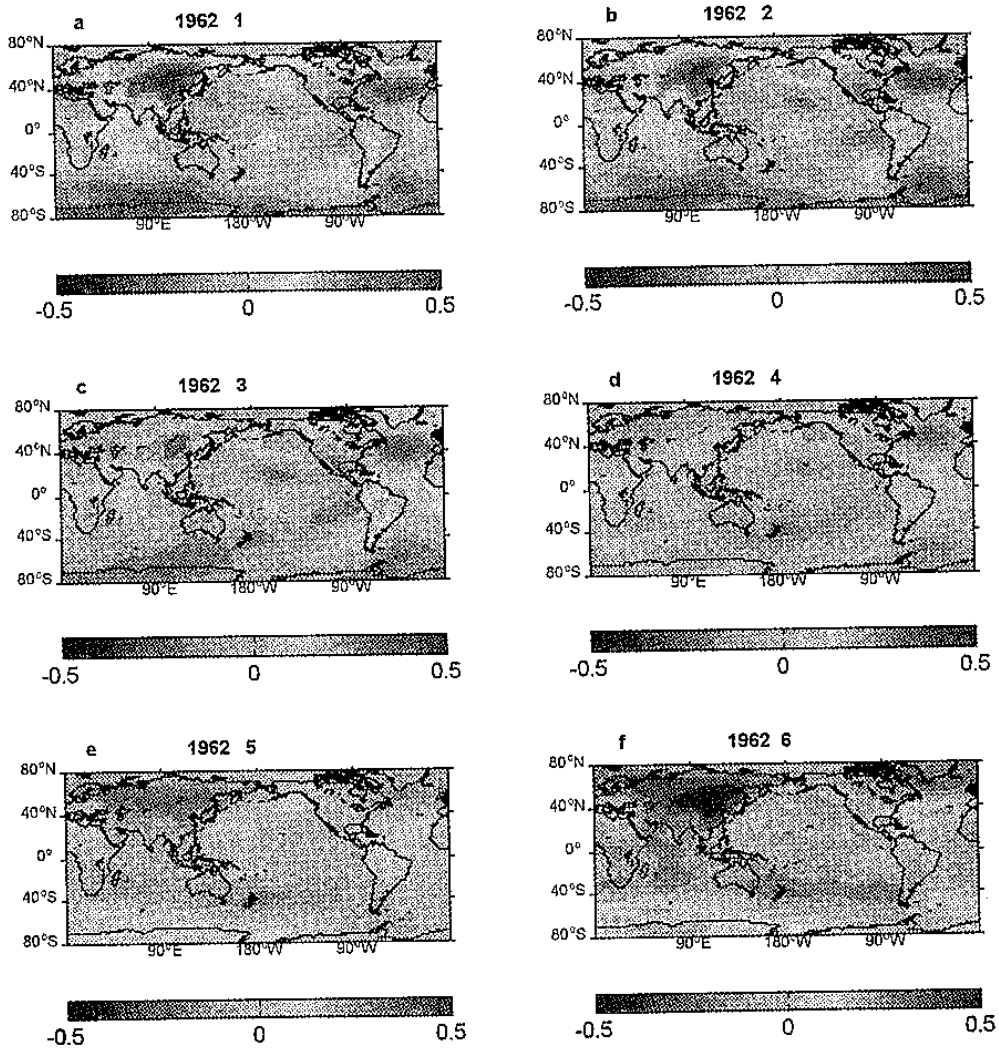


Figure 3. Panel **a** through panel **f** are respectively, reconstructed from ST-PCs 11 and 12 as well as their associated ST-EOFs, the 1,000 hpa geopotential height field from January through June 1962. They represent a half cycle spatial-temporal QAO evolution of geopotential height field. The other half cycle is very similar to these panels except for sign reversal. Thus a complete cycle evolves like $\mathbf{a} \rightarrow \mathbf{b} \rightarrow \mathbf{c} \rightarrow \mathbf{d} \rightarrow \mathbf{e} \rightarrow \mathbf{f} \rightarrow -\mathbf{a} \rightarrow -\mathbf{b} \rightarrow -\mathbf{c} \rightarrow -\mathbf{d} \rightarrow -\mathbf{e} \rightarrow -\mathbf{f}$ . The color bar in each panel represents the range of the normalized amplitude. For example, a grid with 0.5 color scale means that it has amplitude equal to 0.5 of its standard deviation.

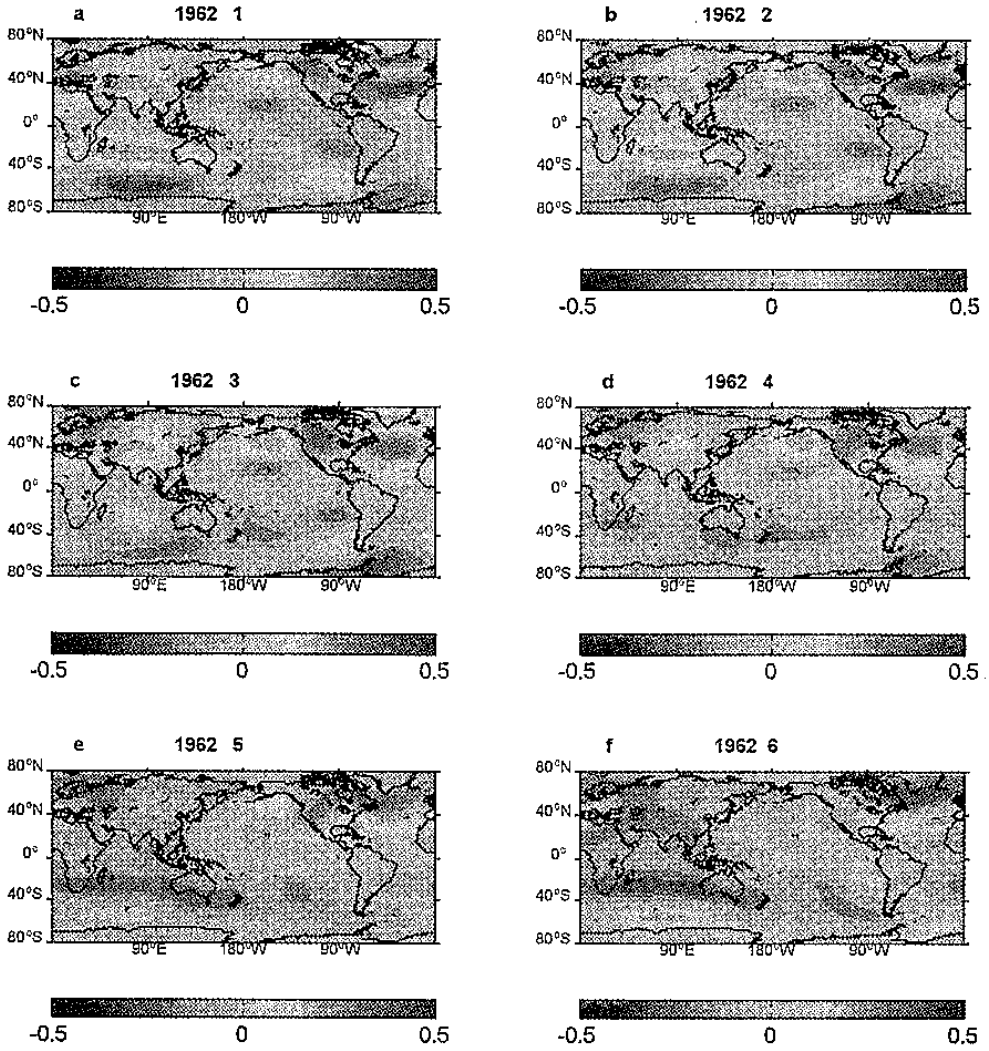


Figure 4. Same as figure 3, except for the geopotential height field at 500 hPa.